remote sensing

MDPI

Article

Validation of Multisource Altimeter SWH Measurements for Climate Data Analysis in China's Offshore Waters

Jingwei Xu [1,2,3,*], Huanping Wu [4], Xiefei Zhi [1], Nikolay V. Koldunov [5], Xiuzhi Zhang [4], Ying Xu [6], Yangyang Zhang [1], Maohua Guo [2], Lisha Kong [4] and Klaus Fraedrich [3]

1 Key Laboratory of Meteorological Disaster, Ministry of Education (KLME)/Joint International Research Laboratory of Climate and Environment Change (ILCEC)/Collaborative Innovation Center on Forecast and Evaluation of Meteorological Disasters (CIC-FEMD)/Joint Center for Data Assimilation Research and Applications, Nanjing University of Information Science and Technology (NUIST), Nanjing 210044, China; zhi@nuist.edu.cn (X.Z.); zhangyy@nuist.edu.cn (Y.Z.)
2 Key Laboratory of Space Ocean Remote Sensing and Application, Ministry of Natural Resources, Beijing 100081, China; gmh@mail.nsoas.org.cn
3 Max Planck Institute for Meteorology, Bundesstrasse 53, 20146 Hamburg, Germany; klaus.fraedrich@mpimet.mpg.de
4 National Climate Centre, Beijing 100081, China; wuhp@cma.gov.cn (H.W.); zxz@cma.gov.cn (X.Z.); kongls@cma.gov.cn (L.K.)
5 Alfred Wegener Institute (AWI), 27568 Bremerhaven, Germany; nikolay.koldunov@awi.de
6 National Satellite Ocean Application Service, Ministry of Natural Resources, Beijing 100081, China; xuying@mail.nsoas.org.cn
* Correspondence: xujw@nuist.edu.cn

Abstract: Climate data derived from long-term, multisource altimeter significant wave height (SWH) measurements are more valuable than those obtained from a single altimeter source. Such data facilitate exploration of long-term air–sea momentum transfer and more comprehensive investigation of weather system dynamics processes over the ocean. Despite the deployment of the first satellite in the Chinese Haiyang-2 (HY-2) series more than 12 years ago, validation and integration of SWH data from China's offshore waters, derived using Chinese altimeters, have been limited. This study constructed a high-resolution, long-term, multisource gridded SWH climate dataset using along-track data from the HY-2 series, CFOSAT, Jason-2, Jason-3, and Cryosat-2 altimeters. Validation against observations from 31 buoys covering China's offshore waters indicated that the SWH variances from HY-2A, HY-2B, HY-2C, CFOSAT, and Jason-3 altimeters correlated well with observations, with a temporal correlation coefficient of approximately 0.95 (except HY-2A, correlation: 0.89). These SWH measurements generally showed a robust linear relationship with the buoy data. Additionally, cross-calibration between Jason-3 and the HY-2A, HY-2B, HY-2C, and CFOSAT altimeters also demonstrated a typically linear relationship for SWH > 6.0 m. Using this relationship, the SWH data were linearly corrected and integrated into a 10 d mean, long-term, multisource altimeter gridded SWH dataset. Compared with in situ observations, the merged 10 d mean SWHs are more accurate and closely match the observations, with temporal correlation coefficients improving from 0.87 to 0.90 and bias decreasing from 0.28 to 0.03 m. The merged gridded SWHs effectively represent the local spatial distribution of SWH. This study revealed the importance of observational data in the process of merging and recalibrating long-term multisource altimeter SWH datasets, particularly before their application in specific ocean regions.

Keywords: merged long-term multisource altimeter data; significant wave height; Haiyang-2 series satellites; CFOSAT; validation; variance; China's offshore waters

Citation: Xu, J.; Wu, H.; Zhi, X.; Koldunov, N.V.; Zhang, X.; Xu, Y.; Zhang, Y.; Guo, M.; Kong, L.; Fraedrich, K. Validation of Multisource Altimeter SWH Measurements for Climate Data Analysis in China's Offshore Waters. *Remote Sens.* **2024**, *16*, 2162. https://doi.org/10.3390/rs16122162

Academic Editor: Sergei Badulin

Received: 8 May 2024
Revised: 4 June 2024
Accepted: 12 June 2024
Published: 14 June 2024

1. Introduction

Historically, marine observational data have had limited availability. Traditionally obtained as ship-based measurements, such datasets were characterized by sporadic spa-

tiotemporal coverage and modest volume. Furthermore, significant wave height (SWH) over sea was generally assessed via visual inspection from commercial marine vessels. The advent of satellite remote sensing technology has revolutionized marine data acquisition, providing rapid, extensive, and synchronous dynamic observations. Specifically, altimeter technology facilitates the retrieval of SWH data. The SWH is calculated as the mean of the highest one-third of waves in a sample. This parameter plays a critical role in understanding air–sea interactions, but it is also crucial for marine meteorology, climatology, and engineering applications [1–3]. The first map of satellite-derived SWH data was based on measurements obtained using the GEOS-3 altimeter in April 1975 [4,5], followed by other sets of SWH data obtained using various spaceborne altimeters. Given the finite operational lifespan of satellite-borne instruments (typically only a few years [6]), together with the narrow viewing swath of a nadir-looking altimeter (approximately 10 km in the footprint), construction of a long-term, high-accuracy gridded climate dataset necessitates integration of multiple data sources. This approach can compensate for the limitations of individual instruments and extends the utility of the derived SWH datasets for ongoing scientific analyses [7].

Satellite radar altimetry has provided global observations of SWH for over 30 years. Following the acquisition of the initial dataset using the GEOS-3 altimeter [4], an array of satellite-borne altimeters has become available, including TOPEX/Poseidon (T/P), the European Remote Sensing Satellite (ERS-1/2), Environmental Satellite (ENVISAT), the Jason series [8], and Sentinel-3A/B [4], in addition to China's Haiyang-2 series (HY-2A/B/C/D) [9]. The China–France Oceanography Satellite (CFOSAT), developed by the China National Space Administration and the Centre National D'Etudes Spatiales (CNES) of France [10], is the first satellite capable of simultaneous global observations of sea surface wind and waves [11–13]. It was launched on 29 October 2018 [14] and, together with other space-based altimeters launched in recent decades, has been used to obtain SWH with relatively high spatial resolution on the global scale [15,16].

Several agencies provide integrated SWH data obtained by multiple missions. These agencies include Globwave (ftp://ftp.ifremer.fr (accessed on 24 July 2023)), the Radar Altimeter Data System (http://rads.tudelft.nl (accessed on 11 June 2024), https://www.aviso.altimetry.fr (accessed on 11 June 2024)), the American National Satellite Ocean Application Service (NSOAS; http://www.nsoas.org.cn/ (accessed on 11 June 2024)), and the National Oceanic and Atmospheric Administration (https://www.noaa.gov/ (accessed on 11 June 2024)). Moreover, the offshore waters of China are characterized by monsoon influence, with distinct variations in dominant wind direction and atmospheric stability near the sea surface between winter and summer. This leads to a significant variance in SWH between seasons and presents substantial challenges for SWH retrieval data accuracy [3]. Despite the broad range of SWH variances observed in China's offshore waters, none of the above data repositories have conducted systematic validation using in situ observations, nor have they constructed long-term, multisource merged datasets focused specifically on this region. Therefore, the objective of this study was to construct a high-resolution, long-term, multisource gridded SWH climate dataset for China's offshore waters using along-track data acquired using various space-borne altimeters.

The remainder of this paper is structured as follows. Section 2 outlines the validation data and the altimeters used in the long-term multisource SWH merging, and it describes both the validation and the merging methodologies. Section 3 presents the validation results for the SWH measurements of each altimeter against in situ observations, the correction equations for each altimeter, the accuracy of the merged data, the spatial characteristics of the merged SWHs, and the temporal variance features of the SWHs. Finally, the main conclusions and discussion derived are presented in Section 4.

2. Data and Methods

2.1. China's Offshore Buoy Measurements of SWH

For use in this study, SWH observations from buoys in China's offshore waters were obtained from the State Oceanic Administration of China and the China Meteorology Administration. These buoy measurements are recorded at hourly intervals. To mitigate potential issues related to land contamination [17], buoy observations within 25 km of the coastline [18], records exceeding 14 m, and constant SWH observations lasting longer than 24 h were eliminated. The dataset comprises observations from 46 buoys, which collectively extend over nearly the entire coastline of China, thereby providing a representative sample of the offshore conditions influenced by the East Asian winter and summer monsoons (Figure 1). The buoys were divided randomly into two groups for analytical purposes: Group One consisted of 31 buoys (Figure 1; purple dots) used to validate individual altimeter measurements and to develop correction functions, whereas Group Two comprised 15 buoys (Figure 1; red dots) used to assess the quality of the final merged SWH dataset. These buoy observations covered the period from 2015 to the present.

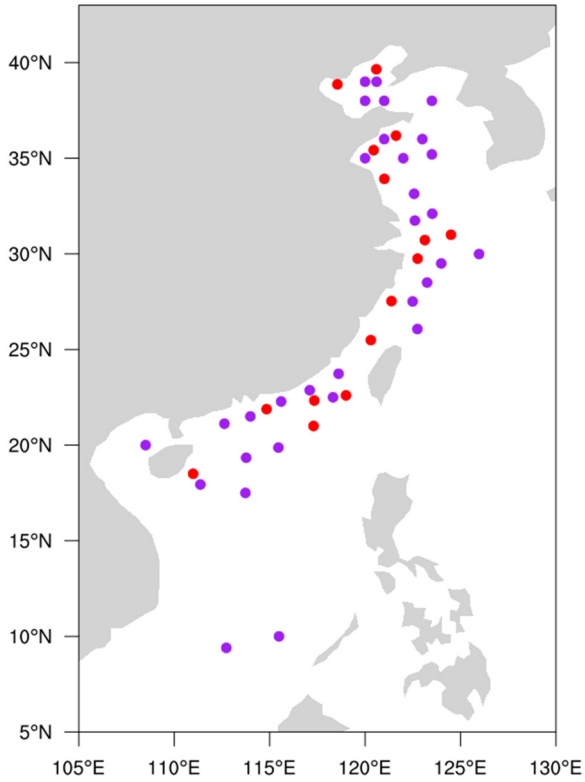

Figure 1. Positions of evaluated buoys in China's offshore waters. Purple dots indicate buoys used for in situ validation, red dots indicate buoys used for validation of the multisource merged SWHs.

2.2. HY-2A SWH Data

The Haiyang-2 (HY-2) satellites are a series of marine dynamic environment remote sensing satellites developed by the NSOAS of China [19]. The Haiyang-2A (HY-2A) satellite is the first of the HY-2 series satellites [20]. The retrieval algorithm for SWH relies on the principle that at near-nadir incidence, the normalized radar cross-section is sensitive to the local slope of the sea waves [21]. It has a dual-frequency radar operating in the Ku and C bands. Ground processing of the data utilizes a four-parameter maximum likelihood estimation retracking algorithm. The root mean square error of HY-2A-derived SWH is 0.30 m after linear correction with in situ SWHs [22]. The SWH data were obtained from the NSOAS website (https://osdds.nsoas.org.cn (accessed on 11 June 2024)).

2.3. HY-2B SWH Data

The Haiyang-2B (HY-2B) satellite is the second in the HY-2 series of marine dynamic environment satellites [23,24]. It has a dual-frequency radar operating in the 13.58 GHz (Ku) and 5.25 GHz (C) bands [25]. Ground processing of the data uses the same four-parameter maximum likelihood estimation retracking algorithm as used for the HY-2A altimeter [26,27]. Geophysical data records were obtained from the NSOAS website (https://osdds.nsoas.org.cn (accessed on 11 June 2024)).

2.4. HY-2C SWH Data

The Haiyang-2C (HY-2C) satellite is the third satellite in the HY-2 series. All the payloads onboard HY-2C are same as those onboard HY-2B, except the radiometer [28]. Unlike HY-2B, which has a sun-synchronous orbit, HY-2C is in a non-sun-synchronous orbit with inclination of 66° and a 10 d repeat cycle [29]. Similar to both HY-2A and HY-2B, the geophysical data records were obtained from the NSOAS website (https://osdds.nsoas.org.cn (accessed on 11 June 2024)). Further information regarding the HY-2 series, CFOSAT, and Jason-3 altimeters used in this study is summarized in Table 1.

Table 1. Information regarding the HY-2 series, CFOSAT, and Jason-3 satellites.

Altimeter	HY-2A	HY-2B	HY-2C	CFOSAT, 2172	Jason-3
Launch Date:	16 August 2011	25 October 2018	21 September 2020	29 October 2018	17 January 2016
Inclination:	99.35°	99.35°	66°	97.5°	66°
Localization:	Sun-synchronous	Sun-synchronous	Non-sun-synchronous, frozen track	Sun-synchronous	Non-sun-synchronous, frozen track
Altitude:	971 km	971 km	957 km	514 km	1336 km

2.5. CFOSAT SWH Data

The Surface Waves Investigation and Monitoring (SWIM) instrument is carried onboard CFOSAT [11–13,21,30,31]. The altimeter-derived nadir SWHs from 29 July 2019 were extracted from the SWIM level 2 product distributed by the AVISO-CNES Data Center in France and the NSOAS in China (ftp://ftp-access.aviso.altimetry.fr/cfosat/ (accessed on 11 June 2024)) [30,32]. To construct a long series of homogenized observations from a large number of altimeter missions, the CFOSAT SWHs were post-calibrated to be unbiased with respect to the Jason-3 mission [27,33] and buoy data at the global scale [34,35]. The Ku band 1 Hz nadir SWHs were also used in this study.

2.6. Jason-3 SWH Data

Jason-3, a successor to the Jason-1, Jason-2, and T/P missions, is an international cooperation satellite altimeter mission among the National Aeronautics and Space Administration, National Oceanic and Atmospheric Administration, the European Organization for the Exploitation of Meteorological Satellites, and CNES. The mission was launched on 17 January 2016. The dual-frequency altimeters in this series, operating in the Ku and C bands, have been used to measure ocean surface topography, SWH, and wind speed.

Jason-3 geophysical data records are distributed by archiving division of CNES. In this study, the SWH data of the Ku band 1 Hz measurements were utilized for the validation and cross-calibration of CFOSAT, HY-2A, HY-2B, and HY-2C data. Similar to the HY-2 series, the four-parameter maximum likelihood estimation retracking algorithm is used for the Jason-3 ground segment reference.

2.7. Jason-2 and Cryoset-2 SWH Data

Given that measurements obtained concurrently from at least three altimeters can be used to construct 10 d mean gridded SWHs [36], but that only HY-2A of the HY series altimeters was available during 2012–2016, we applied Jason-2 and Cryosat-2 as a supplement to construct the 10 d mean gridded SWHs.

Similar to Jason-3, the Jason-2 satellite, a successor to the T/P and Jason-1 altimetry missions, was launched by NASA and the French Space Agency on 20 June 2008. This altimeter has an advanced microwave radiometer onboard, which also operates in the Ku and C bands. The corrected along-track Jason-2 and Cryosat-2 Ku-band 1 Hz SWH data were obtained from the Ifremer database [37].

All the HY-2A, HY-2B, HY-2C, CFOSAT, Jason-2, Jason-3, and Cryosat-2 along-track SWH data used in this study represent 1 Hz Ku-band SWHs. Data filtering was performed before validation, in which SWH records with flags indicating land, ice, and rain were eliminated. The SWH data were carefully checked in the range of 0–14 m.

2.8. Validation Methods

This study analyzed up to 46 buoy measurements for SWH validation. Specifically, 31 buoy observations (Figure 1; purple dots) were utilized for validating single altimeter SWH data and 15 buoy observations (Figure 1; red dots) were used for validating the final merged SWH data. The validation method, as described in [38], employs statistical parameters that include the time series correlation coefficient (R), which is defined by the following equation:

$$R = \frac{\sum_{i=1}^{N} \left(A_i - \overline{A}\right)\left(B_i - \overline{B}\right)}{\sqrt{\sum_{i=1}^{N} \left(A_i - \overline{A}\right)^2 \left(B_i - \overline{B}\right)^2}} \quad (1)$$

where A_i is the altimeter-derived SWH, B_i is the buoy-observed SWH, and N is the number of matched data pairs.

For cross-calibration of the Jason-3 SWHs against the HY-2A, HY-2B, HY-2C, and CFOSAT SWHs, to minimize the impact of sea ice, the collocated SWH data were confined to the region between 60°S and 60°N over the global oceans [24]. The in situ validation method applied temporal and spatial windows of 30 min and 50 km, respectively.

2.9. Method for Merging Long-Term Multisource SWHs

Nadir satellite-derived 1 Hz SWH data were used owing to their lower variability in comparison with that of higher-frequency measurements. The along-track SWH data represent a narrow-view swath of nadir-looking data and provide limited coverage daily SWH measurements of the research area by a single altimeter. Given the spatial coverage and temporal resolution of the final gridded SWHs, we adopted the method of using the 10 d mean SWHs from at least three altimeters [36], and we interpolated these data into gridded boxes with horizontal resolution of 25 km × 25 km. During 2012–2016, among the HY-2 series altimeters, only HY-2A was available; therefore, Jason-2 and Cryosat-2 data were included to satisfy the criterion of using at least three altimeters to construct the 10 d mean gridded SWHs (in Figure 2, the lines indicate the SWHs from an altimeter used in this study). The SWH data of each altimeter were corrected based on in situ observation validation results, and the long-term multisource gridded SWHs were then calculated. Corrections specific to Jason-2 and Cryosat-2 were applied directly using data from the Ifremer database [39].

The study area covered China's offshore waters (0°–43°N, 105°–127°E). The temporal analysis focused on four specific months representative of each season: January for boreal winter, April for spring, July for summer, and October for autumn.

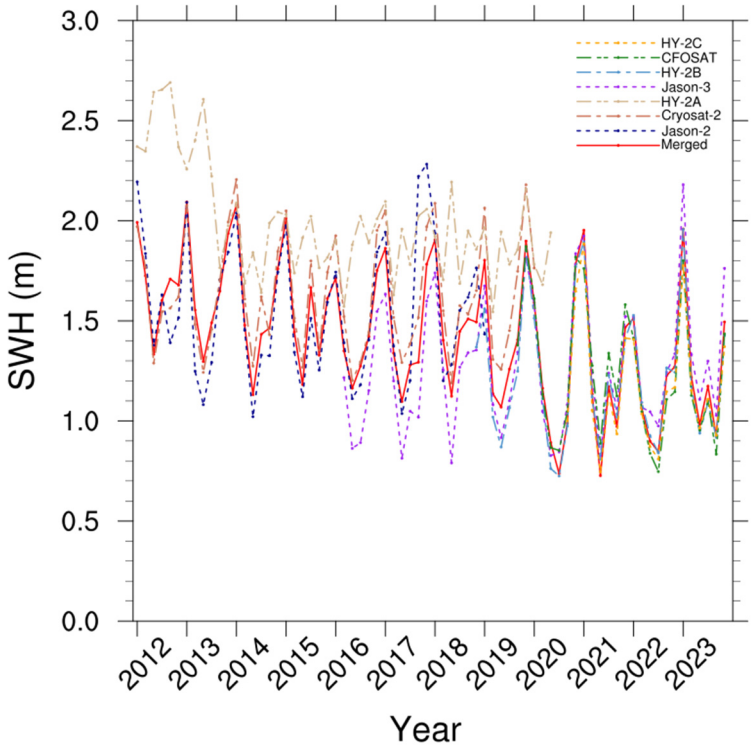

Figure 2. Monthly mean variation in altimeter-derived SWH.

3. Results

3.1. Validation Using In Situ SWHs over China's Offshore Waters

Before utilizing SWH data from altimeters in specific waters, a recalibration process is essential. To accurately reflect the environmental conditions along the entirety of China's offshore waters, 31 uniformly distributed buoys were selected to systematically assess the performance of SWH measurements from the HY-2A, HY-2B, HY-2C, CFOSAT, and Jason-3 altimeters. Comparative results indicate that SWH measurements from those altimeters generally showed reasonable coherence with the buoy observations, with average correlation coefficients of approximately 0.95. However, the HY-2A altimeter produced a lower correlation of 0.89 (Figure 3).

Specifically, SWH data from HY-2A were consistently higher than the buoy measurements. The most closely matched SWH measurements were below 2.3 m, with a time correlation coefficient of 0.89, indicating poorer reliability compared with that of other altimeters. Generally, HY-2A SWH measurements below 1.0 m demonstrated reduced reliability, which contributed to the lower overall correlation coefficient, whereas for measurements above 1.0 m, the accuracy of the HY-2A altimeter was found comparable with that of Jason-2 [20].

The SWH measurements from HY-2B show improved quality compared with those of HY-2A, particularly in the SWH range below 1.0 m (Figure 3b). Generally, SWH values from HY-2B were higher than those observed in all SWH ranges. A high correlation coefficient of 0.97 suggests that the variance in SWH from HY-2B aligns well with the actual sea condition variances, which is consistent with results documented in the American National Data Buoy Center buoys observed SWH comparison [24].

Comparison of SWH data from HY-2C with in situ observation-derived SWH (Figure 3c) reveals a similar pattern to that observed with both HY-2B and HY-2A. Typically, the measurements of SWH from HY-2C were higher than those from the buoy observations. Additionally, the relationship between HY-2C SWHs and the in situ data exhibits a clear linear trend, with a correlation coefficient of 0.96.

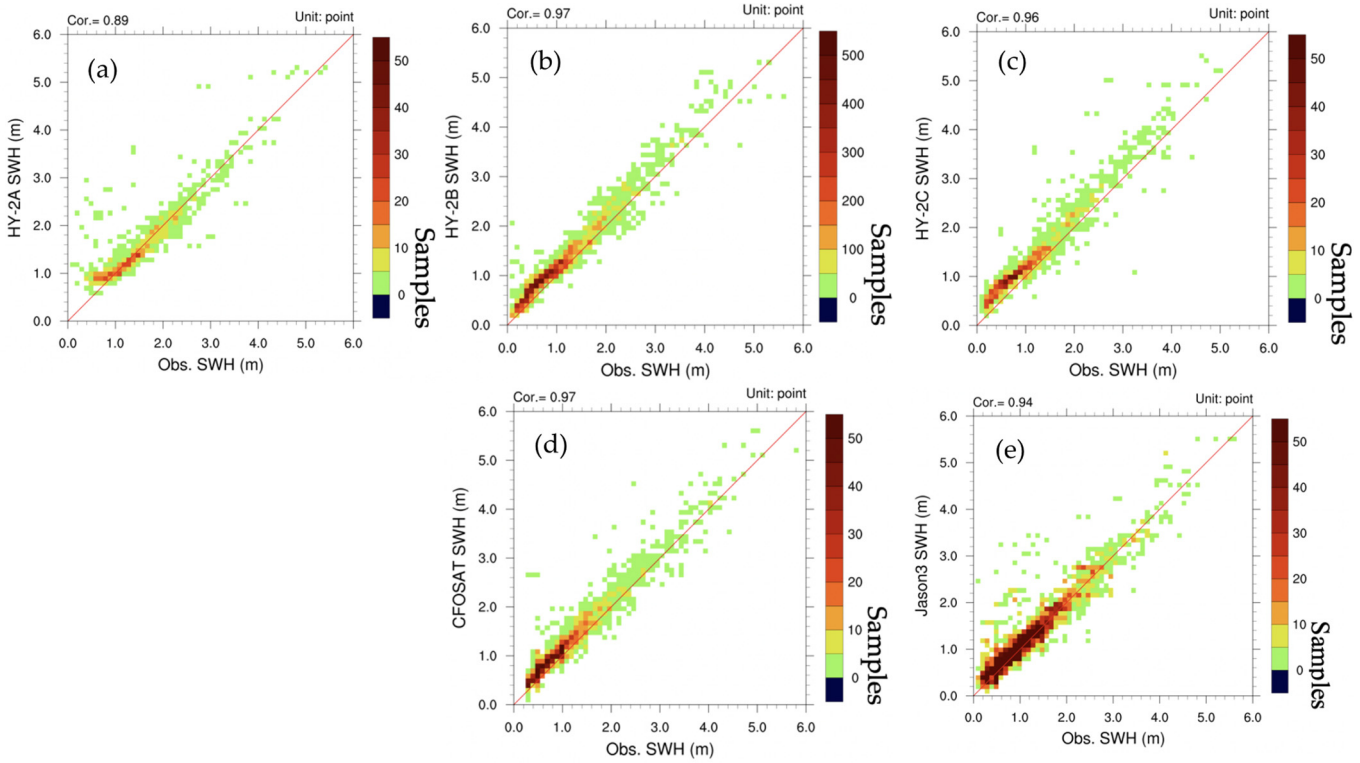

Figure 3. Scatter-point density plots comparing SWH measurements from five altimeters with buoy measurements. The plots show (**a**) HY-2A SWH versus buoy data, followed by similar comparisons for (**b**) HY-2B SWH, (**c**) HY-2C SWH, (**d**) CFOSAT SWH, and (**e**) Jason-3 SWH. The analyses were conducted within temporal and spatial windows of 30 min and 50 km, respectively.

The SWH measurements from CFOSAT show substantial agreement with those from the buoys (Figure 3d). The nadir beam of the SWIM spectrometer onboard CFOSAT operates on the same principle as an altimeter for observing waves and winds [40]. The SWHs measured by SWIM display quality comparable with those measured by both HY-2B and HY-2C, with correlation coefficients of 0.97. This similarity in the strength of the correlation suggests that the quality of SWH measurements from the HY-2 series altimeters is comparable with that of SWHs derived from the CFOSAT altimeter, based on validation of uniform observations.

The matched SWH measurements between Jason-3 and the in situ observations exhibit a strong linear relationship along the $y = x$ line (Figure 3e), indicating a high degree of calibration. However, some SWH measurements plot above the $y = x$ line, suggesting higher values of SWH derived from the altimeter compared with the actual conditions. This disparity suggests that sea conditions in some waters differ markedly from those in areas where the SWHs have been previously calibrated [1,33]. Therefore, a recalibration process is necessary before such measurements can be applied in specific waters.

Overall, comparison of the results from the five altimeters reveals strong correlation with the buoy observations, with an exception for HY-2A SWHs of <1.0 m. The SWH measurements from the HY-2 series are of similar quality to those derived from CFOSAT and Jason-3 in China's offshore waters. The consistent linear relationships observed between all altimeter and buoy measurements indicate that a linear correction equation could be effective for recalibration of SWH measurements from the five altimeters in the specified regions (Table 2). For limited samples in the extreme high SWHs value around 5.0 m, more samples of matched SWHs are needed to draw a solid conclusion.

Table 2. Correction equations and comparison results from the altimeter-derived SWH.

Altimeter, Samples	HY-2A, 1013	HY-2B, 1919	HY-2C, 3461	CFOSAT, 2172	Jason-3, 7919
Bias	−0.01	0.17	0.25	0.17	0.06
Correlation coefficient	0.89	0.97	0.96	0.97	0.94
Linear correction equation	$y = 0.93x + 0.02$	$y = 0.97x - 0.18$	$y = 0.93x - 0.16$	$y = 0.98x - 0.16$	$y = 0.95x - 0.07$

The objective of validating altimeter SWHs against in situ observations is to demonstrate the stability of bias across the range of SWH values. The stable bias characteristics are essential for quality assessment when selecting a reference altimeter during the intercalibration process. To investigate this quality of SWH measurements under different sea conditions, we analyzed the relative bias of SWH measurements from buoys across 0.5 m intervals.

For HY-2A, SWH in the range 1.25–4.75 m displays high quality, with relative bias of approximately −5% (Figure 4a), except in the range 0.25–1.25 m, where the relative bias is as high as 100% for SWH of <0.75 m. The quality improves with increasing SWH; the relative bias is 18% in the 0.75–1.25 m range. Owing to limited sample sizes, data for SWHs of >4.75 m are not sufficiently robust to draw definitive conclusions.

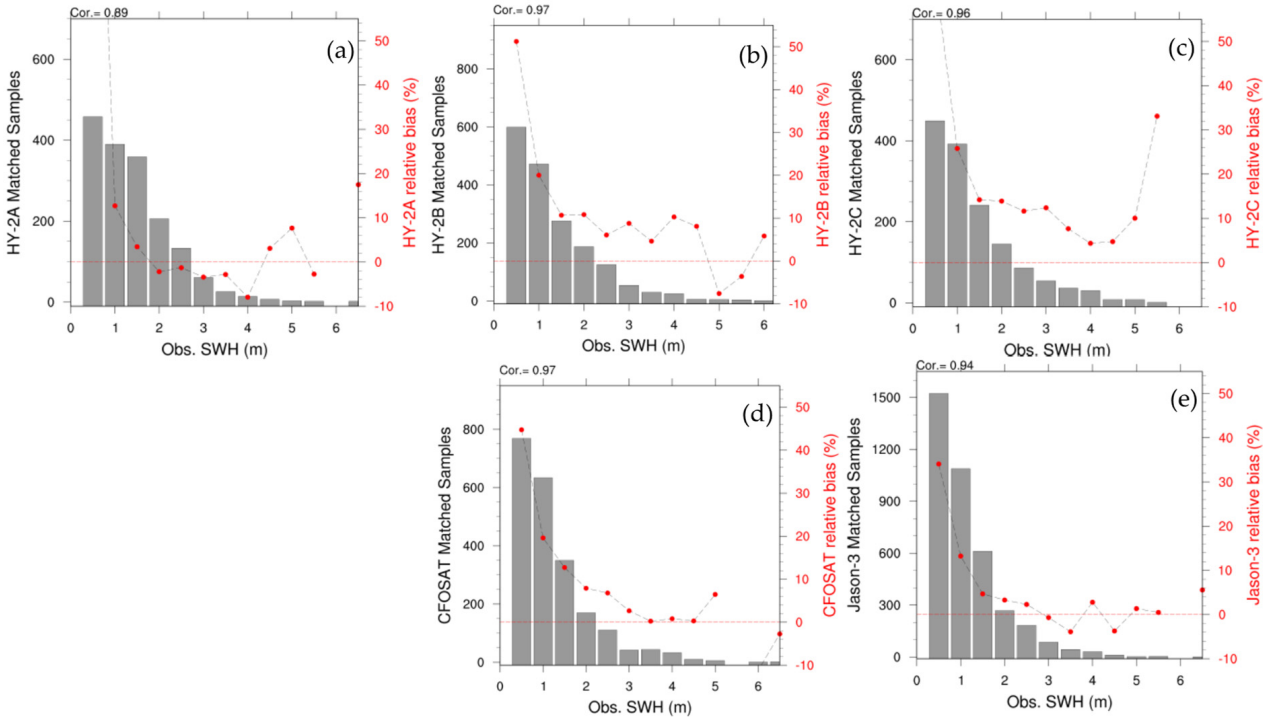

Figure 4. Relative bias of altimeter-derived SWH measurements compared with buoy observations in 0.5 m intervals: (**a**) HY-2A, (**b**) HY-2B, (**c**) HY-2C, (**d**) CFOSAT, and (**e**) Jason-3. The number of samples within each interval (gray columns) is shown on the left-hand *y*-axis, and the relative bias (red dots) is shown on the right-hand *y*-axis.

For HY-2B, the relative bias in SWH in the range of >1.25 m is considered high quality, with relative bias ranging from −10% to 10% (Figure 4b). Similarly, HY-2C shows stable relative bias of approximately 10%, with the highest quality observed in the 3.75–4.75 m range, where the relative bias is 4% (Figure 4c).

The CFOSAT measurements show high quality in the 3.25–4.75 m range, with relative bias near 0% (Figure 4d). However, performance is less satisfactory for SWHs of <1.75 m, where the relative bias exceeds 10%. Jason-3 measurements exhibit a similar distribution of relative bias, demonstrating good calibration in the SWH range of >1.25 m (Figure 4e).

Jason-3 has a non-sun-synchronous orbit, leading to more matched SWHs compared to those from HY-2A and HY-2B.

The distributions of relative bias across different sea conditions indicate varying levels of quality of SWH measurements from the altimeters. In low sea conditions, typically when SWH is <1.25 m, measurements from the altimeters show reasonably low quality. Conversely, in moderate sea conditions, where SWH is in the range 1.75–5.25 m, all altimeters exhibit relative bias of <10%, representing the highest quality among the altimeter measurements. However, only a limited number of samples demonstrate this quality in high sea conditions with SWHs of >6.0 m.

To investigate SWH measurements in open-sea waters and high-sea conditions, specifically where SWH is >6.0 m, we conducted cross-calibration among the altimeters. Notably, Jason-3 and CFOSAT demonstrated stable performance. Given its earlier deployment and longer operational period coinciding with other altimeters, Jason-3 was used as the reference for global ocean cross-calibration between 60°S and 60°N.

In the cross-calibration analysis of the five altimeters, all matched SWH measurements continued to exhibit a linear relationship with Jason-3, indicating uniformity across the observations of the different altimeters (Figure 5a–d). This consistency is also reflected in the relative bias, which maintains a nearly constant linear trend (Figure 5e–h). It is important to note that similar to the in situ calibration results, SWHs of <1.25 m (>1.25 m) from HY-2A are greater (smaller) than those measured by Jason-3. In high-sea conditions with SWHs of >6.0 m, the other altimeters demonstrate a relatively coherent linear relationship with Jason-3.

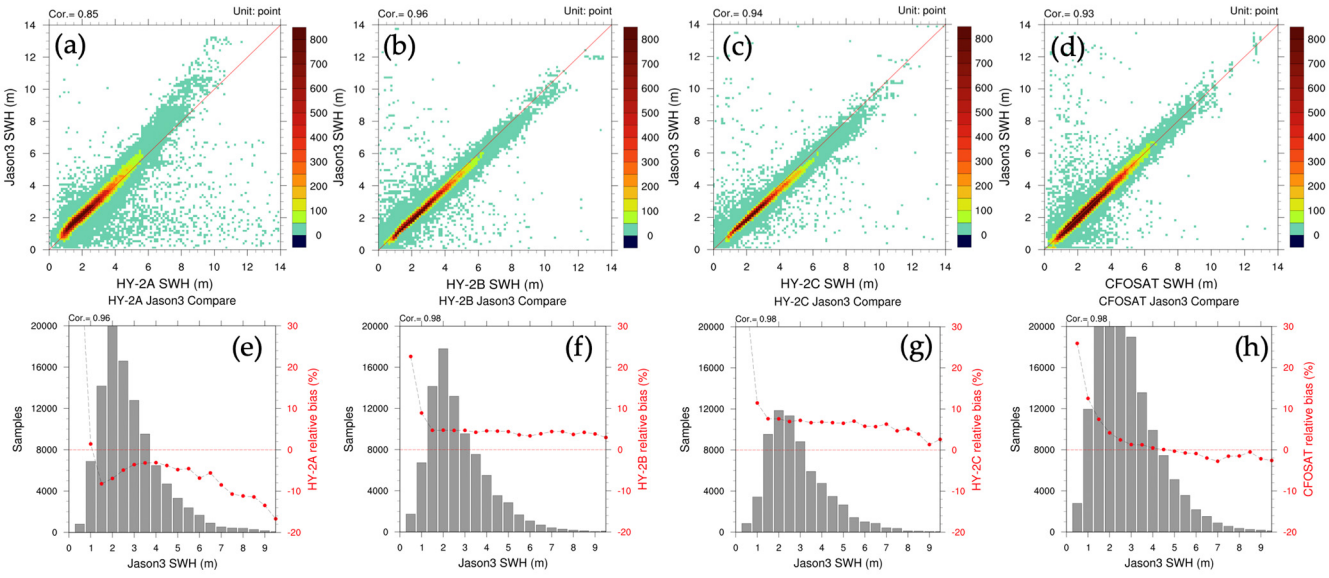

Figure 5. (**a**–**d**) As in Figure 2 but with Jason-3 as reference. (**e**–**h**) As in Figure 3 but with Jason-3 as reference, the number of samples within each interval (gray columns) is shown on the left-hand y-axis, and the relative bias (red dots) is shown on the right-hand *y*-axis. The temporal and spatial windows were 30 min and 50 km, respectively.

3.2. Evaluation of Multisource 10 d Mean Merged SWHs with In Situ SWHs

Owing to the limited spatial distribution of along-track SWH measurements, a merging process is necessary to compile long-term SWH data for China's offshore waters. This process involves combining SWH data from at least three altimeters for each 10 d period [27]. Fifteen additional buoys (indicated by red dots in Figure 1) were utilized to evaluate the quality of the merged SWHs. Double linear interpolation was employed to calculate the gridded SWHs at the buoy locations to obtain the matched SWHs. The buoy data used for validating this dataset are also calculated as a 10 d average.

Analysis of the matched 10 d mean SWHs reveals that the linear-equation-corrected gridded SWHs show improvement over the uncorrected SWHs. The temporal correlation coefficients for the corrected SWHs are 0.9 with bias of 0.03 m (Figure 6a–d), which compare well with the values of 0.87 and 0.28 m, respectively, for the uncorrected SWHs. For the corrected 10 d mean SWHs, the relative bias is between −4% and 3% in the 0.75–3.25 m range and −10% in the 3.25–4.25 m range. These results demonstrate improvement over the uncorrected gridded SWHs, which exhibit relative bias of >10%. This analysis indicates that the linear correction method can effectively enhance the quality of the final averaged gridded SWHs.

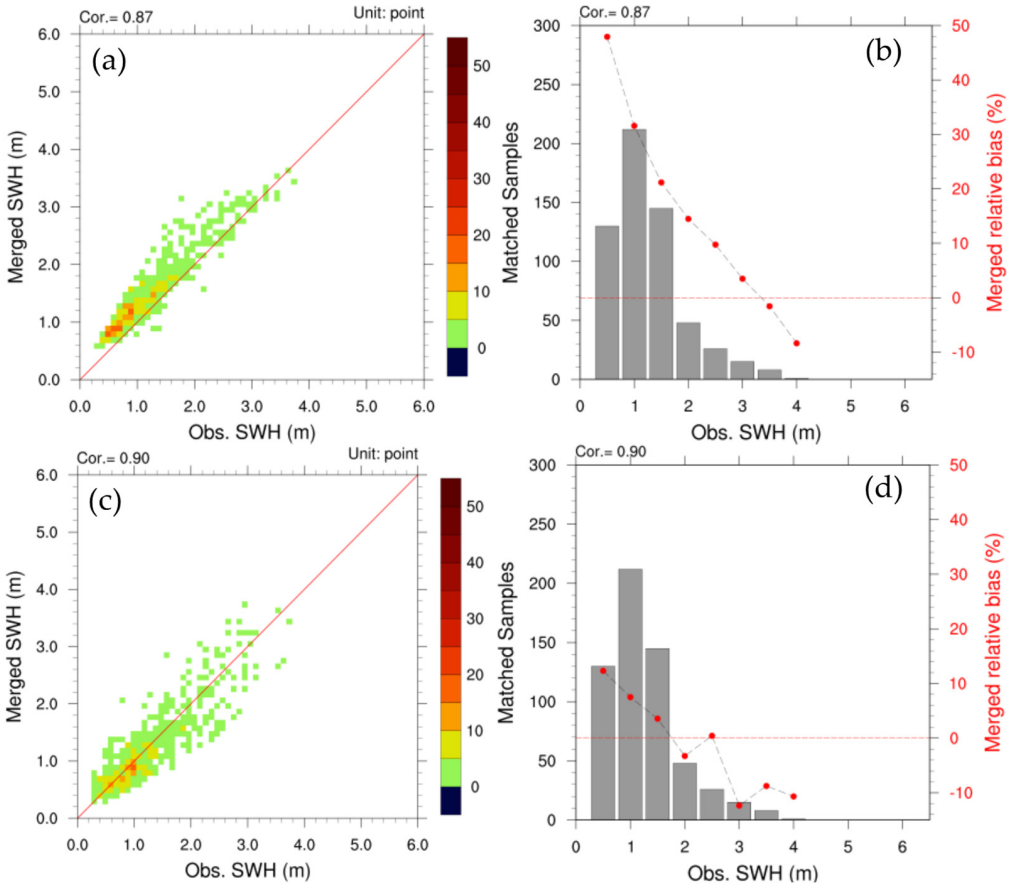

Figure 6. Scatter-point density plots comparing (**a**) the uncorrected 10 d averaged SWH measurements from altimeters with buoy measurements and (**b**) the relative bias of the uncorrected 10 d averaged SWH measurements in 0.5 m intervals with corresponding sample numbers, the number of samples within each interval (gray columns) is shown on the left-hand y-axis, and the relative bias (red dots) is shown on the right-hand *y*-axis. (**c**,**d**) as in (**a**,**b**), respectively, but for the linearly corrected merged SWHs. Compared with the bias in the uncorrected 10 d mean SWHs, the bias in the linearly corrected 10 d mean SWHs decreases from 0.28 to 0.03 m. Considering that the standard deviation (STD) of observations is 0.65, The STD of linearly corrected 10-day averaged SWHs closely matches the observation, with a value of 0.66 m for the corrected dataset compared to an STD of 0.62 m for the uncorrected dataset.

3.3. Spatial and Temporal Characteristics of Merged SWHs

The monthly mean SWHs for January, April, July, and October during 2012–2023 exhibit distinct seasonal variations in China's offshore waters. In January, the region is influenced by the East Asian winter monsoon, with prevailing northeasterly winds that lead to higher SWH values extending from the northeast to the southwest (Figure 7a). In specific areas such as the Taiwan Strait, Bohai Sea, and Beibu Gulf, SWHs might reflect local variations attributable to small-scale sea surface winds.

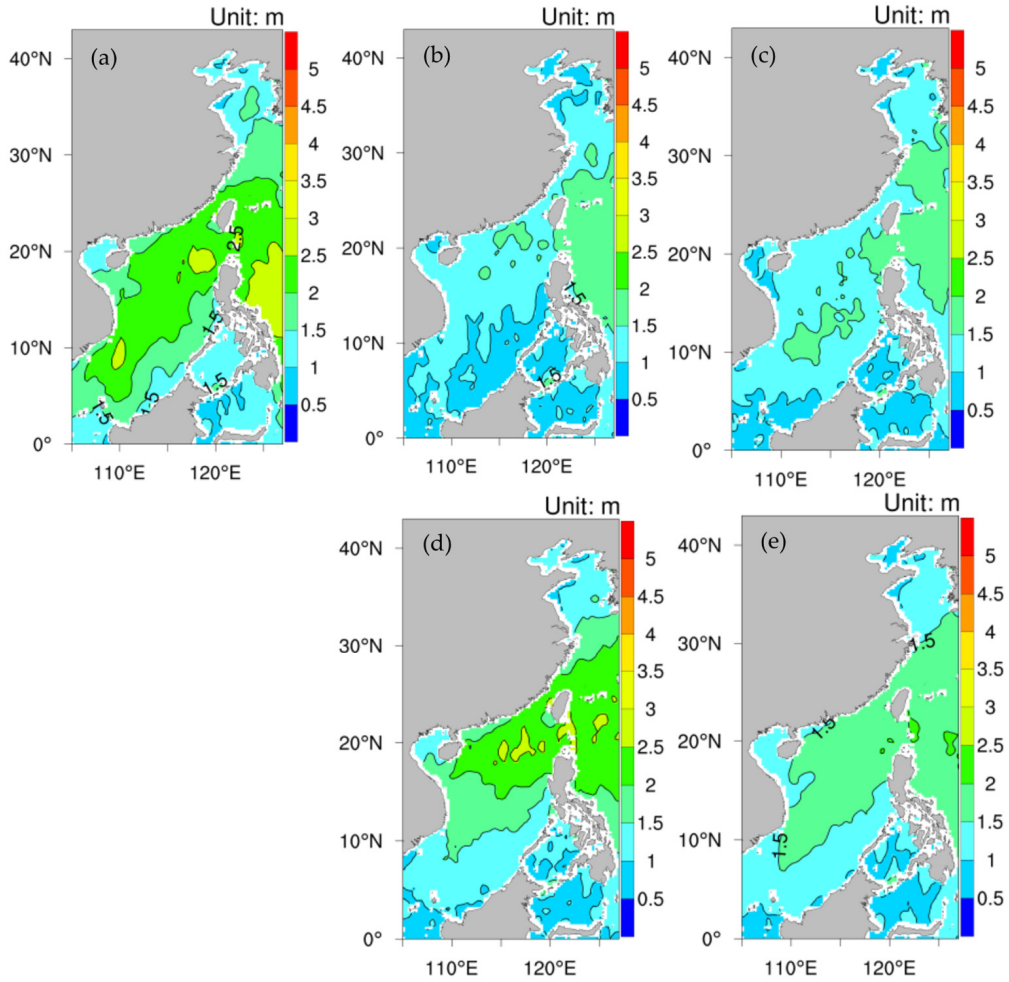

Figure 7. Monthly mean multisource SWHs from 2012 to 2023: (**a**) January, (**b**) April, (**c**) July, (**d**) October, and (**e**) the annual mean.

April marks a transitional period in the seasonal cycle, characterized by relatively low dominant sea surface winds (Figure 7b). Influenced by southern weather systems, southerly winds emerge, resulting in a decrease in SWH from the south to the north in the South China Sea.

In July, all of China's offshore waters are governed by the East Asian summer monsoon and the subtropical high. The result is southerly winds in the South China Sea and southeasterly winds in the Donghai, Huanghai, and Bohai seas that collectively impact SWHs (Figure 7c).

In October, the East Asia winter monsoon resumes its dominance, with the onset of northeasterly winds shaping an SWH pattern similar to that observed in January (Figure 7d).

These four months represent the seasonal dynamics, and the annual mean SWHs (Figure 7e) illustrate the typical fluctuations influenced by the dominant sea surface winds. The spatial distribution and the variances of SWHs are considered reasonable.

The variance of SWHs over time is a critical parameter in oceanographic studies. The monthly mean SWHs in China's offshore waters were analyzed to assess this variance. The averaged SWH data exhibit relatively stable temporal variance. Notably, divergence among the altimeter data has diminished substantially since 2020 owing to improvements in altimeter technology, leading to a marked increase in consistency between altimeter-derived SWHs compared with those obtained in the period 2012–2019 (Figure 1). The averaged SWH values typically lie at the median of the individual altimeter SWH values because they are calculated following correction against the in situ observations. However,

it is important to note that the SWH variances from HY-2A consistently show relatively high bias compared with those of the other altimeters.

4. Conclusions and Discussion

Long-term multisource altimeter-derived merged SWH climate data are more valuable than SWH data from a single altimeter [41]. This is because they allow exploration of long-term air–sea momentum transfer and more comprehensive investigation of weather system dynamics processes over sea. Despite the first of the HY-2 series of Chinese altimeters being in orbit for 12 years and achieving stable observations, which substantially enhances the feasibility of long-term multisource merged SWH studies in China's offshore waters, comprehensive validation of both the altimeters and the SWH products in these regions is lacking. In this study, we validated the SWHs derived from the HY-2A, HY-2B, HY-2C, CFOSAT, and Jason-3 altimeters against in situ observations from 31 buoys distributed uniformly across China's offshore waters. The results demonstrate that the altimeter SWH variances generally align well with the observations, with a temporal correlation coefficient of approximately 0.95 (except HY-2A: 0.89). The matched in situ SWHs and Jason-3 cross-calibration consistently show a robust linear relationship. This linear correction was applied to the SWH data of each altimeter prior to merging. The 10 d averaged SWHs proved to be more precise and more closely aligned with the observations and can effectively represent the local spatial distribution of SWHs. Although this study outlined a method for long-term multisource merging of SWH data, further systematic studies will be necessary to refine the calibration method under anomalous weather conditions. The main findings of this study are summarized in the following.

(1) This study methodically validated SWH measurements from five altimeters across China's offshore waters using 31 buoys. These comparisons demonstrated that linear correction is effective in reducing the bias of each altimeter, although the bias for HY-2A is notably higher for SWHs of <1.0 m, where a nonlinear relationship is observed. In moderate sea conditions, with SWHs of 1.75–5.25 m, all altimeters exhibited a stable relative bias of approximately 10%, indicative of high measurement quality. Correction equations for these altimeters are presented in this paper.

(2) As a supplement to the in situ validation, in scenarios involving open-sea and high-sea conditions with SWHs of >6.0 m, cross-calibration among the multiple altimeters was employed using Jason-3 SWHs as reference. The matched SWHs maintained a linear relationship with Jason-3 and other altimeters, mirrored by consistent relative bias values that were comparable with those of the in situ measurements. These findings indicate that a linear correction equation can effectively minimize biases in the merging method.

(3) Fifteen additional buoys were used to evaluate the quality of the merged SWHs. Validation of the 10 d averaged SWHs against in situ observations indicated improvement in the quality of the corrected gridded SWHs, with temporal correlation coefficients increasing and bias decreasing compared with those of the uncorrected SWHs, exhibiting a reduced bias of 0.03 m compared with a bias of 0.28 m for the uncorrected data.

(4) Analyses of SWHs in four representative months and the annual mean highlighted the influence of dominant sea surface winds across different seasons, accurately reflecting the typical variances of SWHs in China's offshore waters. The spatial distribution and variances of SWHs effectively mirror the real sea conditions. Notably, post-2020, the consistency in the variance among the altimeter-derived SWHs has improved substantially compared with that in 2012–2019, underscoring enhanced measurement reliability over time.

This study focused on the development and analysis of a long-term, multisource altimeter-derived merged SWH product and its spatial and temporal characteristics in relation to China's offshore waters. The linear corrected method is applied in this study, and it performs well in the middle SWHs range 0.75–4.25 m, while in the low SWHs

range < 0.75 m and high SWHs range > 4.25 m, the performance is not as good as that in the middle range. So, it is important to note that extreme weather systems, which can induce high-sea conditions, might impact the results. Despite the relatively limited number of observations, comparisons from 46 buoys moored in China's offshore waters and cross-calibration results between the altimeters consistently demonstrated a linear relationship among the most closely matched SWHs. This finding underscores the need for special attention regarding the variance in the accuracy of merged SWHs under different seasonal conditions in such complex sea environments. Advances in multisource merging approaches, including the use of deep learning techniques, the extension of time series to obtain the linear trends of SWHs in the context of climate change, and the pursuit of higher temporal resolution, such as using daily gridded SWH data, represent promising areas for further development of the proposed method.

Author Contributions: J.X. initiated and coordinated the work. H.W. provided the calculation and validation. J.X., N.V.K. and Y.Z. wrote the manuscript. H.W., X.Z. (Xiefei Zhi), X.Z. (Xiuzhi Zhang), Y.X., Y.Z., M.G., L.K. and K.F. gave valuable suggestions for revisions. X.Z. (Xiefei Zhi) revised the analysis. All authors have read and agreed to the published version of the manuscript.

Funding: This research was jointly supported by project entitled "Research on 8-42d Subseasonal Multi-mode Integrated Forecasting Based on Statistical Methods and Machine Learning" supported by the National Natural Science Foundation of China (grant numbers 42275164 and 41005057), project 2023CFO018 supported by the Key Laboratory of Space Ocean Remote Sensing and Application, MNR, project the China Special Fund for Meteorological Research in the Public Interest (Grant No. GYHY 201406008), and project S1 (Diagnosis and Metrics in Climate Models) of the Collaborative Research Centre TRR 181 Energy Transfer in Atmosphere and Ocean program funded by the German Research Foundation (project 274762653). This study was also funded by "the Priority Academic Program Development of Jiangsu Higher Education Institutions" (PAPD). Also, we acknowledge the High Performance Computing Center of Nanjing University of Information Science & Technology for their support of this work.

Data Availability Statement: The datasets generated for this study are available on request to the corresponding author.

Acknowledgments: We thank anonymous reviewers for comments and suggestions that helped to improve the manuscript. Also, we thank CNSA and CNES for providing the CFOSAT data, NSOAS for providing the HY-2A, HY-2B, and HY-2C data, global altimeter SWH Ifremer database for providing Jason-2 and Cryosat-2 data and SOAC and CMA for providing the buoy observations.

Conflicts of Interest: The authors declare no conflict of interest.

References

1. Sun, M.; Du, J.; Yang, Y.; Yin, X. Evaluation of Assimilation in the MASNUM Wave Model Based on Jason-3 and CFOSAT. *Remote Sens.* **2021**, *13*, 3833. [CrossRef]
2. Xu, J.; Zhi, X.; Sein, D.V.; Cabos, W.; Luo, Y.; Zhang, L.; Dong, F.; Fraedrich, K.; Jacob, D. Predictability of Coastal Boundary Layer Jets in South China Using Atmosphere–Ocean Coupling. *J. Geophys. Res. Atmos.* **2023**, *128*, e2023JD039184. [CrossRef]
3. Xu, J.; Koldunov, N.V.; Remedio, A.; Sein, D.; Zhi, X.; Jiang, X.; Xu, M.; Zhu, X.; Fraedrich, K.; Jacob, D.J.C.D. On the role of horizontal resolution over the Tibetan Plateau in the REMO regional climate model. *Clim. Dyn.* **2018**, *51*, 4525–4542. [CrossRef]
4. Donlon, C.; Berruti, B.; Buongiorno, A.; Ferreira, M.-H.; Féménias, P.; Frerick, J.; Goryl, P.; Klein, U.; Laur, H.; Mavrocordatos, C. The global monitoring for environment and security (GMES) sentinel-3 mission. *Remote Sens. Environ.* **2012**, *120*, 37–57. [CrossRef]
5. Dobson, E.; Monaldo, F.; Goldhirsh, J.; Wilkerson, J. Validation of Geosat altimeter-derived wind speeds and significant wave heights using buoy data. *J. Geophys. Res. Ocean.* **1987**, *92*, 10719–10731. [CrossRef]
6. Quartly, G.D.; Chen, G.; Nencioli, F.; Morrow, R.; Picot, N. An Overview of Requirements, Procedures and Current Advances in the Calibration/Validation of Radar Altimeters. *Remote Sens.* **2021**, *13*, 125. [CrossRef]
7. Timmermans, B.W.; Gommenginger, C.P.; Dodet, G.; Bidlot, J.R. Global Wave Height Trends and Variability from New Multimission Satellite Altimeter Products, Reanalyses, and Wave Buoys. *Geophys. Res. Lett.* **2020**, *47*, e2019GL086880. [CrossRef]
8. Durrant, T.H.; Greenslade, D.J.; Simmonds, I. Validation of Jason-1 and Envisat remotely sensed wave heights. *J. Atmos. Ocean. Technol.* **2009**, *26*, 123–134. [CrossRef]
9. Ribal, A.; Young, I.R. 33 years of globally calibrated wave height and wind speed data based on altimeter observations. *Sci. Data* **2019**, *6*, 77. [CrossRef]

10. Xiang, K.; Yin, X.; Xing, S.; Kong, F.; Li, Y.; Lang, S.; Gao, Z. Preliminary Estimate of CFOSAT Satellite Products in Tropical Cyclones. *IEEE Trans. Geosci. Remote Sens.* **2022**, *60*, 4203516. [CrossRef]
11. Aouf, L.; Dalphinet, A.; Hauser, D.; Delaye, L.; Tison, C.; Chapron, B.; Hermozo, L.; Tourain, C. On the Assimilation of CFOSAT Wave Data in the Wave Model MFWAM: Verification Phase. In Proceedings of the IGARSS 2019—2019 IEEE International Geoscience and Remote Sensing Symposium, Yokohama, Japan, 28 July–2 August 2019; pp. 7959–7961.
12. Hauser, D.; Tourain, C.L.; Hermozo, L.; Alraddawi, D.; Aouf, L.; Chapron, B.; Dalphinet, A.; Delaye, L.; Dalila, M.; Dormy, E.; et al. New Observations from the SWIM Radar On-Board CFOSAT: Instrument Validation and Ocean Wave Measurement Assessment. *IEEE Trans. Geosci. Remote Sens.* **2020**, *59*, 5–26. [CrossRef]
13. Liu, J.; Lin, W.; Dong, X.; Lang, S.; Yun, R.; Zhu, D.; Zhang, K.; Sun, C.; Mu, B.; Ma, J.; et al. First Results From the Rotating Fan Beam Scatterometer Onboard CFOSAT. *IEEE Trans. Geosci. Remote Sens.* **2020**, *58*, 8793–8806. [CrossRef]
14. Xu, Y.; Liu, J.; Xie, L.; Sun, C.; Liu, J.; Li, J.; Xian, D. China-France Oceanography Satellite (CFOSAT) simultaneously observes the typhoon-induced wind and wave fields. *Acta Oceanol. Sin.* **2019**, *38*, 158–161. [CrossRef]
15. Jin, S.; Yang, S.; Yan, Q.; Jia, Y. Significant Wave Height Estimation from CYGNSS Delay-doppler Map Average Observations. In Proceedings of the 2022 Photonics & Electromagnetics Research Symposium (PIERS), Hangzhou, China, 25–29 April 2022; pp. 654–659.
16. Ren, L.; Yang, J.; Xiao, Q.; Zheng, G.; Wang, J. On CFOSAT swim wave spectrometer retrieval of ocean waves. In Proceedings of the 2017 IEEE International Geoscience and Remote Sensing Symposium (IGARSS), Fort Worth, TX, USA, 23–28 July 2017; pp. 1966–1969.
17. Zhang, K.; Dong, X.; Zhu, D.; Yun, R. Estimation and Correction of Geolocation Errors of the CFOSAT Scatterometer Using Coastline Backscatter Coefficients. *IEEE J. Sel. Top. Appl. Earth Obs. Remote Sens.* **2021**, *14*, 53–61. [CrossRef]
18. Hall, C.; Jensen, R.E. *Utilizing Data from the NOAA National Data Buoy Center*; U.S. Army Corps of Engineers/Engineering Research and Development Center: Vicksburg, MS, USA, 2021.
19. Ye, X.; Lin, M.; Xu, Y. Validation of Chinese HY-2 satellite radar altimeter significant wave height. *Acta Oceanol. Sin.* **2015**, *34*, 60–67. [CrossRef]
20. Zhang, H.; Wu, Q.; Chen, G. Validation of HY-2A Remotely Sensed Wave Heights against Buoy Data and Jason-2 Altimeter Measurements. *J. Atmos. Ocean. Technol.* **2015**, *32*, 1270–1280. [CrossRef]
21. Hauser, D.; Tison, C.; Amiot, T.; Delaye, L.; Corcoral, N.; Castillan, P. SWIM: The First Spaceborne Wave Scatterometer. *IEEE Trans. Geosci. Remote Sens.* **2017**, *55*, 3000–3014. [CrossRef]
22. Chen, C.; Zhu, J.; Lin, M.; Zhao, Y.; Wang, H.; Wang, J. Validation of the Significant Wave Height Product of HY-2 Altimeter. *Remote Sens.* **2017**, *9*, 1016. [CrossRef]
23. Wang, J.; Aouf, L.; Jia, Y.; Zhang, Y. Validation and Calibration of Significant Wave Height and Wind Speed Retrievals from HY2B Altimeter Based on Deep Learning. *Remote Sens.* **2020**, *12*, 2858. [CrossRef]
24. Jia, Y.; Yang, J.; Lin, M.; Zhang, Y.; Ma, C.; Fan, C. Global assessments of the HY-2B measurements and cross-calibrations with Jason-3. *Remote Sens.* **2020**, *12*, 2470. [CrossRef]
25. Li, X.; Xu, Y.; Liu, B.; Lin, W.; He, Y.; Liu, J. Validation and Calibration of Nadir SWH Products from CFOSAT and HY-2B with Satellites and In Situ Observations. *J. Geophys. Res. Ocean.* **2021**, *126*, e2020JC016689. [CrossRef]
26. Xu, X.-Y.; Xu, K.; Shen, H.; Liu, Y.-L.; Liu, H.-G. Sea Surface Height and Significant Wave Height Calibration Methodology by a GNSS Buoy Campaign for HY-2A Altimeter. *IEEE J. Sel. Top. Appl. Earth Obs. Remote Sens.* **2016**, *9*, 5252–5261. [CrossRef]
27. Yang, J.; Zhang, J.; Jia, Y.; Fan, C.; Cui, W. Validation of Sentinel-3A/3B and Jason-3 Altimeter Wind Speeds and Significant Wave Heights Using Buoy and ASCAT Data. *Remote Sens.* **2020**, *12*, 2079. [CrossRef]
28. Wang, J.; Yu, T.; Deng, F.; Ruan, Z.; Jia, Y. Acquisition of the Wide Swath Significant Wave Height from HY-2C through Deep Learning. *Remote Sens.* **2021**, *13*, 4425. [CrossRef]
29. Qin, D.; Jia, Y.; Lin, M.; Liu, S. Performance Evaluation of China's First Ocean Dynamic Environment Satellite Constellation. *Remote Sens.* **2023**, *15*, 4780. [CrossRef]
30. Jiang, H.; Mironov, A.; Ren, L.; Babanin, A.V.; Wang, J.; Mu, L. Validation of Wave Spectral Partitions from SWIM Instrument On-Board CFOSAT Against In Situ Data. *IEEE Trans. Geosci. Remote Sens.* **2022**, *60*, 4204013. [CrossRef]
31. Liang, G.; Yang, J.; Wang, J. Accuracy Evaluation of CFOSAT SWIM L2 Products Based on NDBC Buoy and Jason-3 Altimeter Data. *Remote Sens.* **2021**, *13*, 887. [CrossRef]
32. Li, B.; Li, J.; Liu, J.; Tang, S.; Chen, W.; Shi, P.; Liu, Y. Calibration Experiments of CFOSAT Wavelength in the Southern South China Sea by Artificial Neural Networks. *Remote Sens.* **2022**, *14*, 773. [CrossRef]
33. Tran, N.; Vandemark, D.; Zaron, E.D.; Thibaut, P.; Dibarboure, G.; Picot, N. Assessing the effects of sea-state related errors on the precision of high-rate Jason-3 altimeter sea level data. *Adv. Space Res.* **2021**, *68*, 963–977. [CrossRef]
34. Dodet, G.; Piolle, J.-F.; Quilfen, Y.; Abdalla, S.; Accensi, M.; Ardhuin, F.; Ash, E.; Bidlot, J.-R.; Gommenginger, C.; Marechal, G. The Sea State CCI dataset v1: Towards a sea state climate data record based on satellite observations. *Earth Syst. Sci. Data* **2020**, *12*, 1929–1951. [CrossRef]
35. Han, L.; Ji, Q.; Jia, X.; Liu, Y.; Han, G.; Lin, X. Significant Wave Height Prediction in the South China Sea Based on the ConvLSTM Algorithm. *J. Mar. Sci. Eng.* **2022**, *10*, 1683. [CrossRef]
36. Xu, J.; Wu, H.; Xu, Y.; Koldunov, N.V.; Zhang, X.; Kong, L.; Xu, M.; Fraedrich, K.; Zhi, X. Validation of Nadir SWH and Its Variance Characteristics from CFOSAT in China's Offshore Waters. *Remote Sens.* **2023**, *15*, 1005. [CrossRef]

37. Sepúlveda, H.H.; Queffeulou, P.; Ardhuin, F. Assessment of SARAL/AltiKa Wave Height Measurements Relative to Buoy, Jason-2, and Cryosat-2 Data. *Mar. Geod.* **2015**, *38*, 449–465. [CrossRef]
38. Yang, J.; Zhang, J. Validation of Sentinel-3A/3B satellite altimetry wave heights with buoy and Jason-3 data. *Sensors* **2019**, *19*, 2914. [CrossRef] [PubMed]
39. Queffeulou, P. Long-Term Validation of Wave Height Measurements from Altimeters. *Mar. Geod.* **2004**, *27*, 495–510. [CrossRef]
40. Ren, L.; Yang, J.; Xu, Y.; Zhang, Y.; Zheng, G.; Wang, J.; Dai, J.; Jiang, C.L. Ocean Surface Wind Speed Dependence and Retrieval from Off-Nadir CFOSAT SWIM Data. *Earth Space Sci.* **2021**, *8*, e2020EA001505. [CrossRef]
41. Young, I.R.; Ribal, A. Multiplatform evaluation of global trends in wind speed and wave height. *Science* **2019**, *364*, 548–552. [CrossRef]